HYDRODYNAMICS OF A GAS-LIQUID COLUMN EQUIPPED WITH MELLAPAKPLUS PACKING

E. Brunazzi*#, A. Paglianti*, L. Spiegel, F. Tolaini***

*Laboratory of Process Equipment, Department of Chemical Engineering, Industrial Chemistry and Material Science, University of Pisa, I-56126 Pisa, Italy (#e.brunazzi@ing.unipi.it)
**Sulzer Chemtech Ltd, CH-8404 Winterthur, Switzerland

ABSTRACT

This paper describes the results of an experimental and modelling study on hydrodynamics of MellapakPlus packing operated under counter-current gas-liquid flow. The experimental work was focused on measuring the pressure drop, liquid holdup and capacity limit of this packing at specific liquid loads of up to 80 $m^3/m^2/h$. Experimental results for the air/water system confirm that MellapakPlus packing allows substantial gains in throughput compared to its standard counterpart, Mellapak 250.Y. Experiments were also carried out using aqueous solutions of Carboxymethylcellulose (CMC) as the liquid phase to evaluate the effect of liquid viscosity. A mechanistic model, based on mass- and momentum-conservation equations, is presented for the prediction of the pressure drop up to flooding point.

INTRODUCTION

Packed towers operated under gas-liquid counter current conditions have found increased application in distillation, absorption and liquid-liquid extraction processes. They are also becoming increasingly important in environmental protection technologies [1]. Continued market competition has forced researchers and manufacturers to search for improvements in the design of column internals. Among these, structured packings have received the greatest attention owing to their good performance. It is well recognised, in fact, that structured packings can save energy and reduce column dimension by offering high mass transfer efficiency at lower energy consumption compared to random packings. Moreover, structured packings are favoured over less expensive trays especially in vacuum to near atmospheric distillation applications where they allow a significant reduction in operating costs to be made due to the lower pressure drop per theoretical stage [2, 3].

Standard structured packings are made of corrugated sheets or gauzes arranged in parallel with oppositely oriented flow channels inclined at an angle of 45 or 60 deg to the horizontal. Such a structure permits a high specific surface to be obtained (250 m^2/m^3 or 500 m^2/m^3 in the most commonly used packings) with void fractions of about 98%. The gauze packing BX, developed by Sulzer 30 years ago, and the sheet metal packing Mellapak 250.Y, introduced by Sulzer in late 1970s can be considered the predecessors of a number of structured packings such as Montz B1 and C1 types (by the Montz Company), Gempak packings (by Glitsch Inc.), RaluPak (by Raschig Company) and Flexipac (by Koch).
Continued market demand for increased capacity and/or efficiency has forced researchers and manufacturers to search for geometrical improvements in structured packing. Standard sheet metal packings with corrugation angle increased from 45 to 60 deg were introduced (e.g. Sulzer Mellapak X-type). Although this allowed a significant increase in the capacity [4], the percentage of capacity gain was roughly equal to the percentage reduction of mass transfer efficiency [5]. Recent efforts have been directed at conceiving new packing types providing the 45 deg corrugation efficiency while approaching the larger capacity of the 60 deg corrugation. Experimental studies on Mellapak packings [6, 7, 8] revealed that liquid accumulates at the interface between packing elements at gas loads above the loading point. This effect has been identified as a limiting factor for capacity enhancement. Suess and Spiegel [6] showed that flooding in Mellapak starts where two packing elements touch each other (see Figure 1).

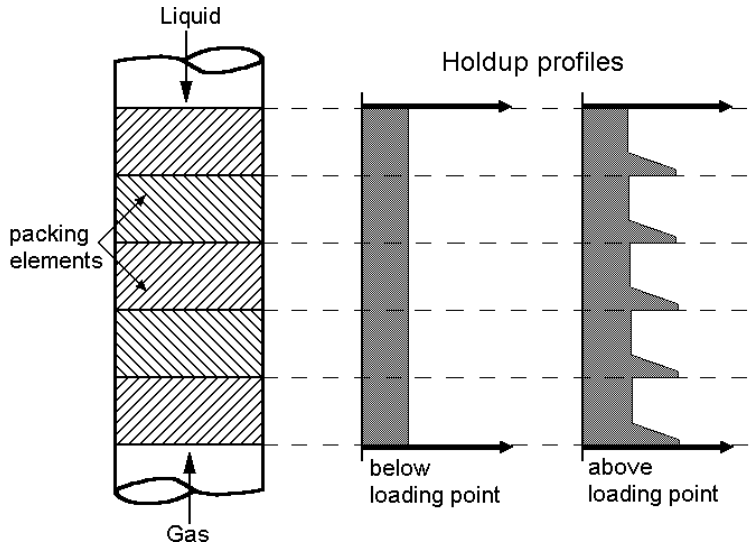

Fig. 1 - Vertical holdup profile of Mellapak below and above loading point

Brunazzi et al. [8] measured local liquid hold-up in Mellapak 250.Y packing using a capacitance probe and they concluded that pressure drop due to the change in the gas flow direction in the zone between two adjacent elements is the main cause of liquid stagnation at operation above loading. In a structured packing bed, packing elements are stacked in a way that each subsequent packing element is rotated with respect to the previous one, normally by 90 deg. This means that the ascending gas is forced to make a sharp change in flow direction at each transition between packing elements [9]. The result is a increase in pressure drop in the zone where two elements touch which causes premature flooding in that zone. Koch-Glitsch Inc. has

introduced Flexipac-HC, based on an invention by Billingham and Lockett [10] and licensed by Praxair. The only difference in this packing from the original Flexipac is in the bottom end of each packing element, where each corrugated sheet has been flattened to provide increased hydraulic diameter and to enable a smoother flow direction change for the gas phase. Similarly, Montz Company recently introduced Montz B1-M, which is the evolution of the Montz B1 series. The major feature is a rather long, smooth bend in the bottom part of the corrugation with continuously increasing corrugation base width [5].
Sulzer Chemtech has introduced MellapakPlus packing [11]. This packing differs from its conventional Mellapak counterpart in that at the top and bottom ends of each packing element the corrugations are bent to the vertical, creating a smooth transition zone between the elements (see Fig. 2). The gas flow remains at 45 deg in the main part of the packing. At the upper and lower ends, where the elements meet, the flow is now vertical instead of following a right angle, thereby reducing the gas velocity by about 25%. The change in gas flow direction is now steady and smooth unlike the abrupt change found in conventional Mellapak. The published performance curves [12], show that these modifications have enabled capacity to be increased without affecting separation efficiency.

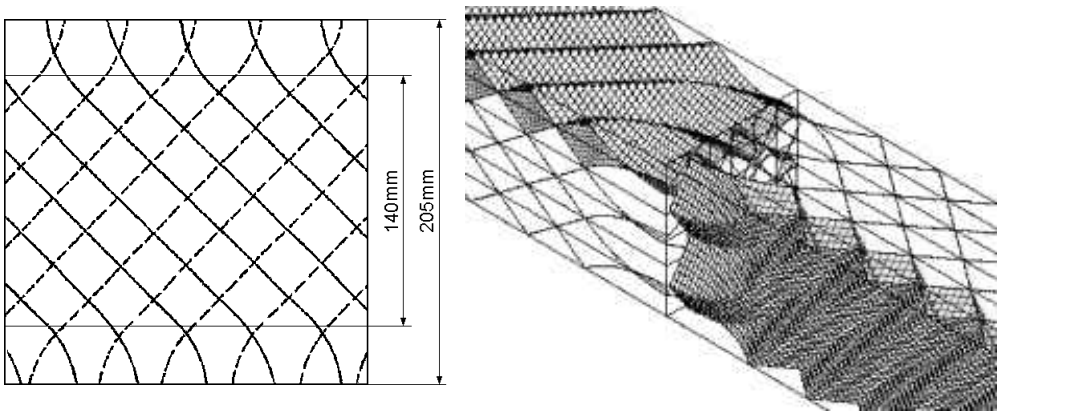

(from [11])

Fig. 2 - Schematic illustration of MellapakPlus design

No experimental data from independent sources have been published so far in open literature. The present work reports a comprehensive study on the hydrodynamics of this MellapakPlus packing. New experimental data were obtained for liquid hold-up, pressure drop and capacity limit over a wide range of liquid loads. Experiments were also carried out using aqueous solutions of Carboxymethylcellulose (CMC) to evaluate the effect on hydrodynamic performance of liquid viscosity.

EXPERIMENTS

Experimental Device and Measurements

The experiments presented in this paper were carried out in the test rig situated at the Department of Chemical Engineering, Industrial Chemistry and Materials Science of the University of Pisa (Italy). A sketch of the experimental setup is shown in Figure 3. The pilot column is 6700 mm high and has an inner diameter of 400 mm. It is equipped with 14 stainless steel elements of MellapakPlus 252.Y, which have been

arranged to give a total bed height of 2870 m. Each element is placed with a rotation of 90 deg with respect to adjacent elements to assure better radial mixing.
The main characteristic dimensions of the MellapakPlus 252.Y packing are a specific surface area, a_g, of 256 m^2/m^3 and a void fraction, e, of 0.988.

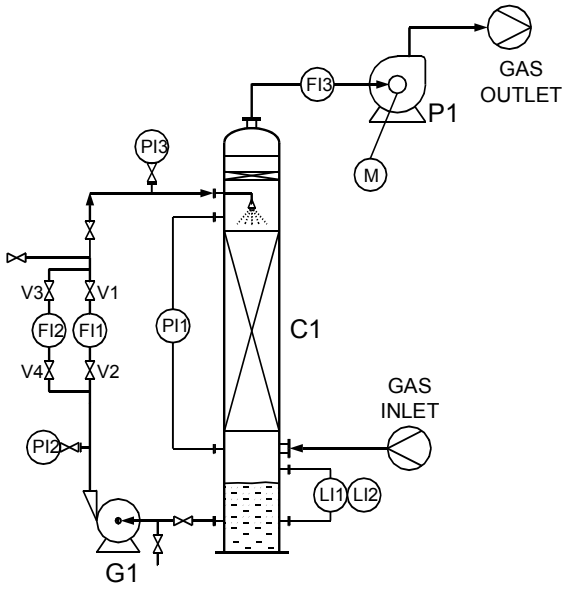

Fig. 3 - Experimental setup

Air at room conditions is used, and is driven by a fan, which permits flow rates of up to 2500 Nm^3/h. The column works in counter current operation of gas and liquid. The gas flow rate is measured with an orifice meter and adjusted by acting on the inverter of the fan motor.
The liquid follows a closed circuit. A centrifugal pump circulates the liquid from the bottom to the top of the column with a specific liquid load of up to 80 $m^3/m^2/h$. Entering at the top of the column, the liquid is distributed over the packing by solid cone spray nozzles type CP, manufactured by Caccialanza & C. srl (Milan, Italy) and suitable for use over the range of liquid loads employed, then it flows down over the packing and back into the sump.
Water was used as the liquid for these experiments. To obtain higher viscosities without affecting the other physical properties of the liquid (i.e. density and surface tension), aqueous solutions of CMC were also used. CMC aqueous solutions at 1.78 and 3.06 wt% were used which had liquid viscosities of 5 and 14 cP respectively. Carbofix 5A type CMC sold by Barzaghi srl (Milan, Italy) was used to prepare the solutions. All tests were carried out under atmospheric conditions.
Each test began by pumping the liquid over the packing to ensure thorough wetting of the packing. The liquid flow was then stopped for a while to allow excessive liquid to drain from the packing. After setting the desired liquid load, the gas flow rate was increased in steps up to flooding condition, while readings were taken of pressure drop over the bed and liquid level in the column sump.
The pressure drop over the bed was measured both by a Differential Pressure Transmitter and by a U-tube manometer filled with water. The liquid level in the column sump was measured by a Differential Pressure Transmitter.
The dynamic liquid hold-up was determined by volumetric balance measurement [13]: the decrease of the liquid level in the column sump was used to determine the

liquid hold-up of the packing. Particular care was used to assure that steady state was reached before each measurement. The static hold-up was measured together with corresponding empty column hold-up values in a separate experiment.

Experimental Results

Figure 4 shows an example of the data obtained in the present work using air/water and air/CMC solutions as working fluids [14]. Figure 4a shows the experimental pressure drop against the gas load (in terms of the F-factor) at room conditions for a liquid load of 32 $m^3/m^2/h$. The corresponding liquid hold-up data are given in Figure 4b. From the experimental data, liquid hold-up without gas flow is found to increase with the viscosity of the liquid phase. This means that for a given liquid load, the cross section available for the gas flow decreases if the viscosity of the liquid phase increases and hence the pressure drop increases as shown in Figure 4a. Figure 4b shows that for a given liquid load, the effect of liquid viscosity is to anticipate the flooding point.

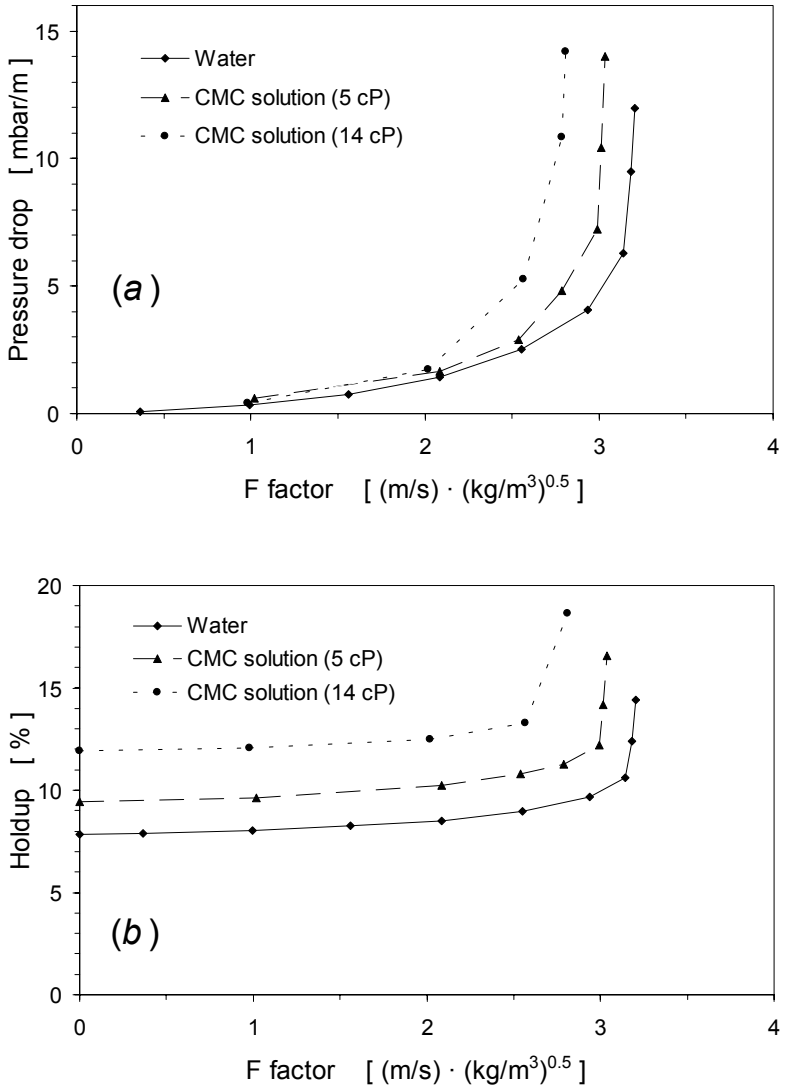

Fig. 4 Pressure drop (a) and liquid hold-up (b) vs. F factor. Effect of liquid viscosity (liquid load: 32 $m^3/m^2/h$)

Figure 5 compares the pressure drop versus F-factor for MellapakPlus and Mellapak 250.Y. The data for Mellapak 250.Y packing were taken from Meier et al. [15]. The figure highlights that for similar liquid loads, the MellapakPlus packing allows a reduction in pressure drop compared with the Mellapak 250.Y and that the flooding point shifts to higher gas F factors.

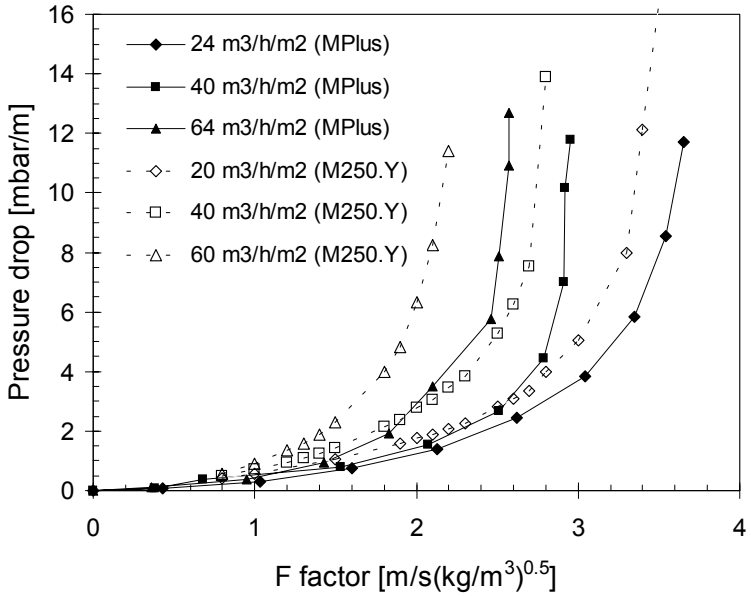

Fig. 5 Pressure drop vs. F factor. Comparison between MellapakPlus (present data) and Mellapak 250.Y (from Meier et al. [15])

One of the most important design factors of a packed column is its capacity. The gas capacity of a column is limited by the onset of flooding. Flooding conditions can be defined in different ways: (a) when the slope of the pressure drop curve goes to infinity, (b) when the efficiency goes to zero, (c) when mean liquid hold-up increases by a factor of 2-3. As pointed out by Spiegel and Meier [4], the onset of flooding is very difficult to measure, therefore they suggested using the concept of a capacity limit which is defined simply as the point of operation where pressure drop equals 12 mbar/m. According to Spiegel and Meier [4], the capacity of a column can be represented on a Wallis-type diagram. This is a plot of $C_G^{0.5}$ versus $C_L^{0.5}$ where

$$C_G = U_{sg} \cdot \left(\frac{\rho_g}{\rho_l - \rho_g} \right)^{0.5} \quad (1)$$

$$C_L = U_{sl} \cdot \left(\frac{\rho_l}{\rho_l - \rho_g} \right)^{0.5} \quad (2)$$

U_{sg} and U_{sl} are the superficial gas and liquid velocities respectively, and ρ_g and ρ_l are the gas and liquid densities. The capacity of MellapakPlus 252.Y packing obtained by analysis of the present experimental data is given in Figure 6 in the form of a Wallis diagram. This approach avoids the inclusion of the effect of liquid viscosity in the capacity term, so the figure can highlight the liquid viscosity effect on the flooding

locus by showing the trend for solutions of different viscosity on the same graph. For a fixed liquid load, the gas limit capacity is lower for viscous systems than for air/water system.

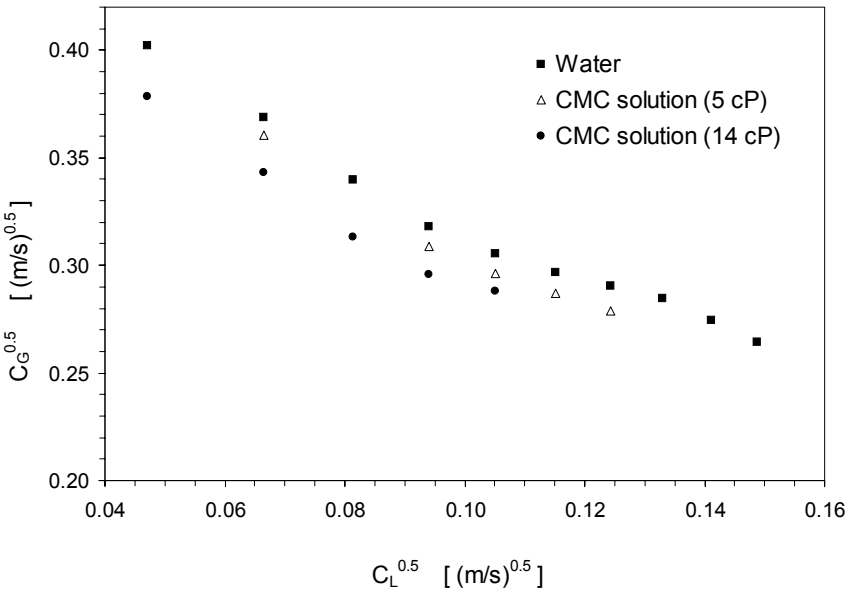

Fig. 6 Capacity of MellapakPlus. Effect of liquid viscosity

Figure 7 compares the capacity of MellapakPlus with that of Mellapak 250.Y. The results refer to the air/water test mixture with different liquid loads.

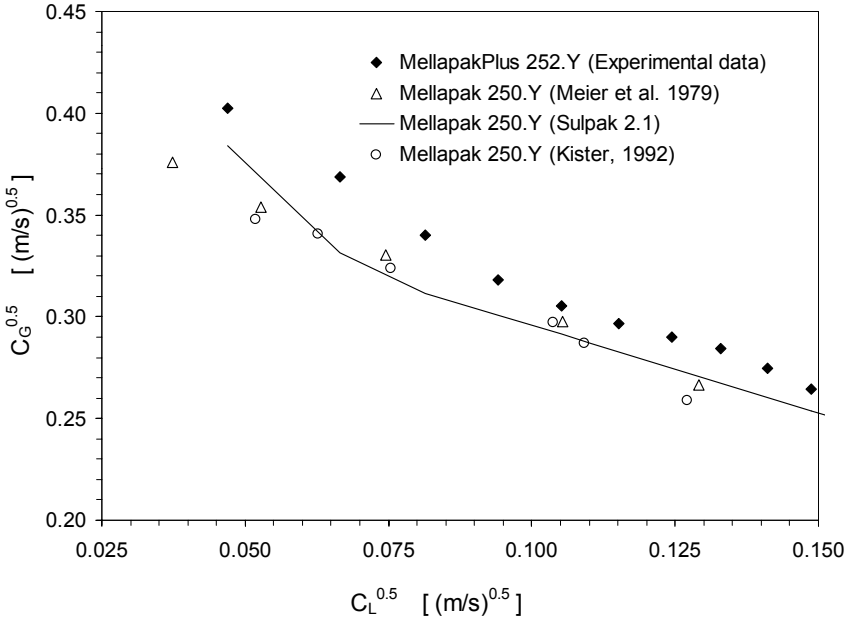

Fig. 7 Capacity of MellapakPlus (present data) and Mellapak 250Y (from Meier et al. [15]; Kister [16]; Sulpak [17]) (air/water system)

The experimental data for Mellapak 250.Y were obtained from Meier et al. [15] and from Billet data published in Kister [16]. The computed capacity data for the Mellapak 250.Y packing were obtained by running Sulzer's Sulpak program (ver2.1) [17] for a column with inner diameter of 0.4 m. The results in Figure 7 clearly show the gain in capacity obtained with MellapakPlus packing compared to its conventional counterpart, Mellapak 250.Y.

Finally, superficial gas velocity at capacity limit for MellapakPlus is compared with the values given for Mellapak 250.Y in the form of a parity plot in Figure 8.

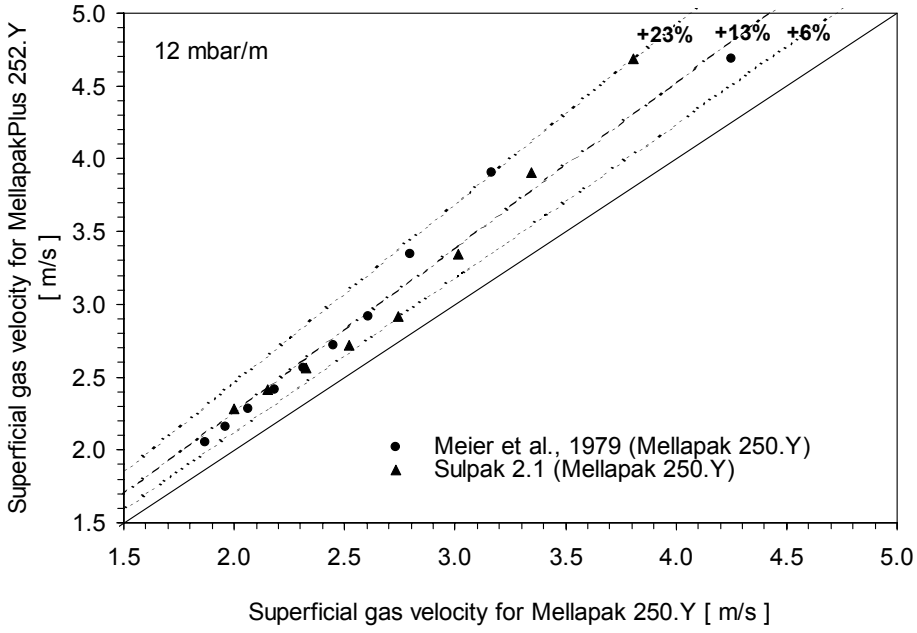

Fig. 8 Comparison of superficial velocity at capacity limit of MellapakPlus (present data) with Mellapak 250Y (from Meier et al. [15]; Sulpak [17]) (air/water system)

The figure highlights that MellapakPlus packing results in a significant enhancement in column capacity over conventional packing. Mean throughput gains of 13% have been obtained over a wide range of liquid loads. It is necessary to point out that this comparison was limited to the air/water system due to an absence in open literature of experimental data for Mellapak 250.Y.

It can be concluded that the results obtained in the present work confirm the validity of the effect of geometrical changes made to the Mellapak packing. The improved MellapakPlus packing shows increased capacity and reduced pressure drop when compared to its counterpart, Mellapak 250.Y.

MECHANISTIC PRESSURE DROP MODEL

Reliable conceptual design models are useful both for new designs and for optimal revamping of existing equipment.
In a previous work [9], the authors developed a model to predict pressure drop and liquid hold-up of conventional structured packing. This is the basis for the present model to predict the hydrodynamics from below loading point up to flooding point of MellapakPlus packing based on the experimental results.

Mechanistic Model

In MellapakPlus packing the liquid flows on the surface of each layer as thin film, while the gas flows through the channels contacting the liquid in a way that can be considered similar to a partially wetted wall arrangement.
The hydraulic scheme used in the present work is based on the assumption that the channels within the packing (see Figure 9) can be approximated to a bundle of identical columns inclined with respect to the horizontal axis by an angle equal to the corrugation angle, ϑ, i.e. by 45 deg.

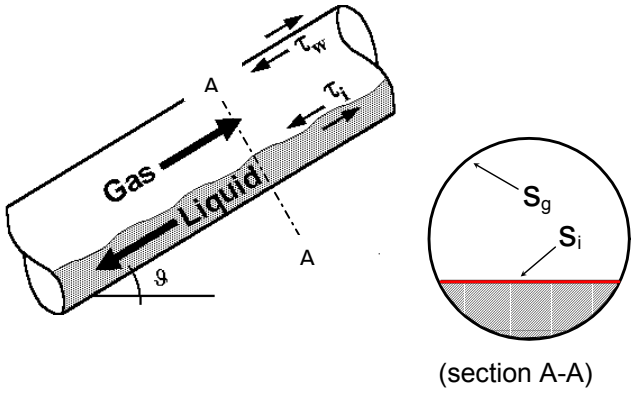

Fig. 9 Simplified scheme of the channel

The main assumptions made to develop the model are that (a) the liquid is Newtonian and flows over the structured packing as a falling film in laminar regime, (b) the two-phase flow pattern is *separate* with the liquid flowing on the bottom of each channel and the gas phase above it.

According to this packing scheme, friction losses arising from the flow of the gas phase through the column can be attributed to two terms. The first term, named distributed frictional losses, takes into account losses at the channel walls and at the gas-liquid interface. The second term considers friction losses resulting from changes in the flow directions at the interface between two adjacent packing elements, and is named concentrated frictional loss. The pressure gradient per unit height of bed is then given by the sum of frictional and gravitational terms, with the assumption that both the liquid and the gas flows remain acceleration free and at steady state and hence the acceleration term is negligible:

$$\left(\frac{dP}{dx}\right) = \left(\frac{dP}{dx}\right)_{F,d} + \left(\frac{dP}{dx}\right)_{F,c} + \left(\frac{dP}{dx}\right)_{G} \qquad (3)$$

The gravitational term, assuming incompressible flow, is simply computed by:

$$\left(\frac{dP}{dx}\right)_G = \rho_g g \qquad (4)$$

The expression for frictional losses is examined in the following sections, while a detailed description of the various terms is given in the Appendix.

Concentrated Frictional Losses (Direction Changes)

A theoretically based approach has been adopted, similar to those developed for simple geometries such as transport pipelines. The concentrated term is evaluated by:

$$\left(\frac{dP}{dx}\right)_{F,c} = 4 f_m \frac{L_{eq}}{d_e} N_c \rho_g \frac{V_g^2}{2} \qquad (5)$$

where f_m is the friction factor (see eq. a11 in Appendix), N_c is the number of flow direction changes per unit height of packing, L_{eq} is the length of channel giving a pressure drop equivalent to that arising from the change in the flow direction due to each single bend, d_e is the characteristic dimension of the flow channel, and V_g is the effective gas velocity in the channel.

According to [9], the number of bends per unit height of packing, N_c, depends on the packing element height, the channel inclination angle and the column diameter. When column diameter is greater than packing height, as in the present case, the number of bends is simply given by the inverse of the packing element height, i.e. $N_c = 1/H$.

In standard structured packing bed, packing elements are stacked in a way that each subsequent packing element is rotated with respect to the previous one, normally by 90 deg. This implies that the ascending gas is forced to make a sharp change in the flow direction at each transition between packing elements. The term L_{ed}/d_e is related to the sharpness of the change in the flow direction of the gas. As shown in a previous work [9], a value of 25 of L_{ed}/d_e was assumed for packing with a 60 deg corrugation angle and of 35 for packing with a 45 deg corrugation angle. MellapakPlus packing differs from its conventional counterpart, the Mellapak 250.Y, in that at the top and bottom ends of each packing element, the corrugations are bent to the vertical, creating a smooth transition zone between the elements. The flow remains at 45 deg in the main part of the packing. At the upper and lower ends, where the elements meet, the flow is vertical instead of following a right angle, and this reduces the gas velocity by about 25%. The change in gas flow direction is now steady and smooth and no longer abrupt as with the conventional Mellapak. A value of 29 of L_{ed}/d_e for the MellapakPlus packing has been obtained from dry pressure drop measurements in the present work.

Distributed Frictional Losses

A momentum balance on the gas phase gives the following expression for the frictional distributed losses per unit height of the packing:

$$\left(\frac{dP}{dx}\right)_{F,d} = \frac{4}{\pi d_e^2 (1 - h_l/e)\cdot \sin\vartheta}\left[\tau_{wg} s_g + \tau_i s_i\right] \tag{6}$$

where τ_i and τ_{wg} are the shear stresses at the gas-liquid interface and at the channel wall respectively, s_i is the length of interfacial chord and s_g is the channel perimeter affected by the gas flow (see Figure 9). In the present model it is assumed that the length of interfacial chord is equal to the length of the channel perimeter wetted by the liquid. Therefore, both s_i and s_g are simple functions of the wetted specific surface area a_e. The present model assumes that the wetted area depends on the liquid load but is not significantly influenced by the gas load [7, 18], and both the gas-liquid interfacial chord and the channel perimeter are not affected by the gas flow and depend exclusively on the liquid load.

If the gas and liquid effective velocities remain constant along the column, and the liquid is Newtonian and flows under laminar conditions, the momentum equation on the falling liquid film can be integrated giving the film thickness:

$$\delta = \frac{\frac{\tau_i}{2\mu_l} + \sqrt{\left(\frac{\tau_i}{2\mu_l}\right)^2 + 4\left(\rho_l g\sin\vartheta - \left(\frac{dP}{dy}\right)_{chan}\right)\frac{V_l}{3\mu_l}}}{\frac{2}{3\mu_l}\left[\rho_l g\sin\vartheta - \left(\frac{dP}{dy}\right)_{chan}\right]} \tag{7}$$

where

$$\left(\frac{dP}{dy}\right)_{chan} = \left(\frac{dP}{dx}\right)_{F,d}\sin\vartheta + \rho_g g\sin\vartheta \tag{8}$$

Pressure Drop per Unit Height of Packing

Finally, the pressure drop per unit height of the packing can be computed as:

$$\left(\frac{dP}{dx}\right)_T = \frac{4}{\pi d_e^2 (1 - h_l/e)\cdot \sin\vartheta}\left[\tau_{wg}\pi d_e\left(1 - \frac{a_e}{a_g}\right) + \tau_i \pi d_e\left(\frac{a_e}{a_g}\right)\right] + 4f_m \frac{L_{eq}}{d_e} N_c \rho_g \frac{V_g^2}{2} + \rho g \tag{9}$$

Method of Solution

For a given liquid load, to solve the model we need to perform an iterative procedure to evaluate shear stresses and liquid film thickness, and hence liquid hold-up at varying gas loads. The input variables to be fed to the model are: liquid hold-up in absence of gas flow, fluid superficial velocities, physical properties of the fluids, bed and packing characteristics.

Validation of Model

This section compares results from the mechanistic model with experimental results. As an example, Figure 10 shows a comparison of experimental and computed data for pressure drop versus the gas F factor at varying liquid loads for the air/water system.

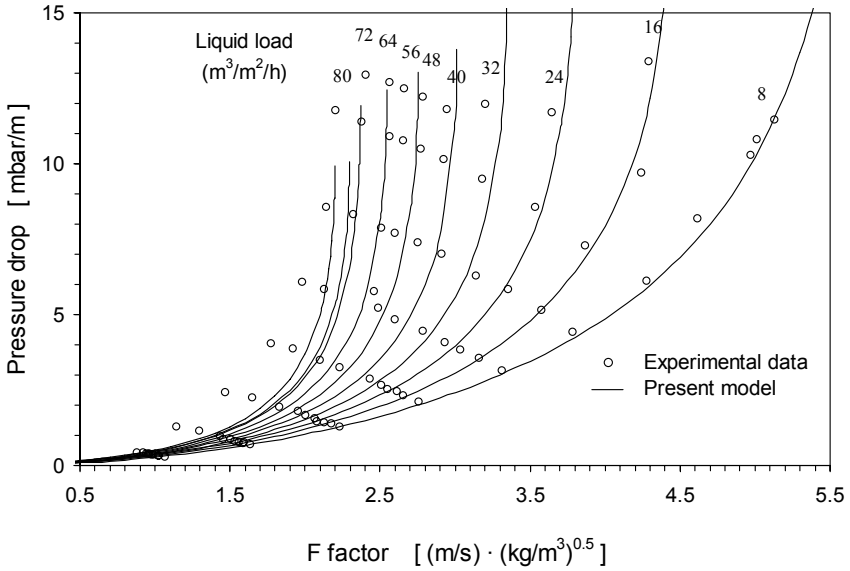

Fig. 10 Pressure drop vs F factor. Comparison between experimental and computed data (air/water system)

A very good agreement is found between predicted and measured pressure drop for liquid loads up to 48 $m^3/m^2/h$. For higher liquid loads, the model tends to underpredict measured pressure drop in the loading zone although the flooding point is satisfactorily predicted.

Figure 11 compares the experimental and the computed capacity of the MellapakPlus packing for all the systems tested in the present work. The figure shows that the model makes a good prediction of the experimental data and enables the effect of liquid viscosity to be taken into account.

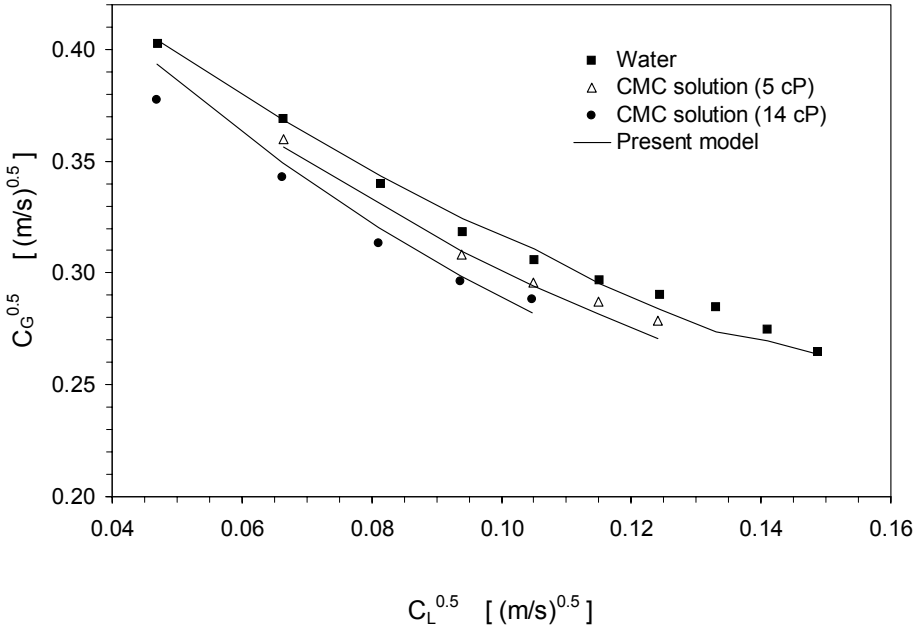

Fig. 11 Capacity of MellapakPlus.
Comparison of experimental and computed data

Finally, the quality of the model prediction is shown in Figure 12 where a parity plot of computed and measured values of gas capacity is given for all the tested systems. The figures highlight that the data are within the $\pm 5\%$ band.

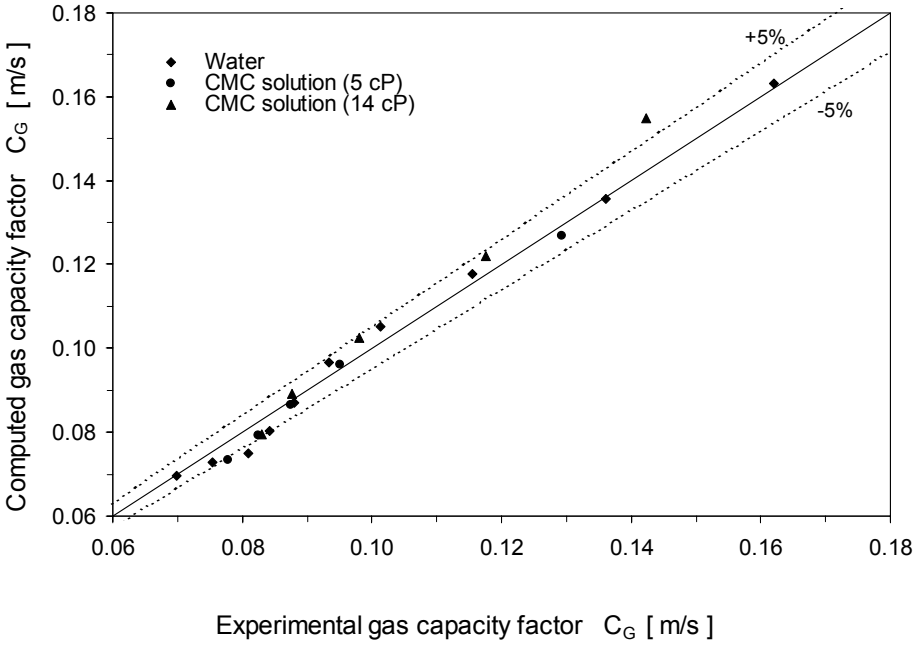

Fig. 12 Capacity of MellapakPlus. Comparison of experimental and computed gas capacity factors at capacity limit

CONCLUSIONS

In the present work, hydrodynamic experiments were carried out to investigate the performance of MellapakPlus packing. New experimental data were obtained on liquid holdup, pressure drop and capacity limit over a wide range of liquid loads. The experimental data confirm the enhanced performance of the packing compared to its conventional counterpart, Mellapak 250.Y. The influence of liquid viscosity on hydrodynamic performance was also investigated using aqueous solutions of CMC.
A mechanistic model based on mass- and momentum-conservation equations was developed to predict pressure drop and flooding in MellapakPlus packing. This is based on a design model developed previously by the authors in the study of conventional structured packing. The predictive accuracy of the model was tested by comparing experimental and computed data. The satisfactory results highlight that the proposed model could be a useful tool both for design and revamping of existing equipment.

APPENDIX

Interfacial Chord and Fractional Dry Perimeter

According to the present hydraulic model, shear stresses both at the channel walls and at the gas-liquid interface contribute to the frictional losses, and to evaluate them, knowledge of both the gas-interfacial area and of the unwetted fraction of the channel wall is necessary. According to the packing scheme, the interfacial chord and the channel perimeter affected by the gas phase are simple functions of the packing fractional wetted area:

$$s_i = \pi d_e \left(a_e / a_g\right) \tag{a1}$$

$$s_g = \pi d_e - s_i \tag{a2}$$

where d_e is the packing characteristic dimension defined as [19]

$$d_e = 4e / a_g \tag{a3}$$

As shown in previous work [2, 9], fractional wetted area of the packing is related to the liquid hold-up measured without gas flow. The starting point of the approach is the assumption that the liquid is Newtonian and flows on the structured packing as a falling film in laminar conditions. With these assumptions, the momentum equation on the falling liquid film in absence of gas flow can be written as:

$$\left(\frac{\partial \tau_{zy}}{\partial z}\right) = \rho_l g \sin\vartheta \tag{a4}$$

which in the integrated form gives the film thickness:

$$\delta = \sqrt{\frac{3\mu_l U_{sl}}{h_l (\sin\vartheta)^2 \rho_l g}} \tag{a5}$$

The film thickness is related to the liquid hold-up by

$$h_l = \frac{s_i \delta e}{\pi d_e^2 / 4} \qquad \text{(a6)}$$

Thus, substitution of eq.a1 and eq.a2 into eq.a6 gives a relation between fractional wetted area and liquid hold-up measured in the absence of gas flow.

Shear Stresses and Friction Factors

The shear stresses at the wall and at the gas-liquid interface are given respectively by:

$$\tau_{wg} = \frac{1}{2} f_g \rho_g V_g^2 \qquad \text{(a7)}$$

$$\tau_i = \frac{1}{2} f_i \rho_g \left(V_g^2 + V_l^2 \right) \qquad \text{(a8)}$$

where the effective gas, V_g, and liquid, V_l, velocities can be evaluated as:

$$V_g = \frac{U_{sg}}{(e - h_l)\sin\vartheta} \qquad \text{(a9)}$$

$$V_l = \frac{U_{sl}}{h_l \sin\vartheta} \qquad \text{(a10)}$$

and the friction factor, f_m, derives from a mean, weighted on the wetted area, between the wall friction factor, f_g, and interfacial friction factor, f_i.

$$f_m = f_i \frac{a_e}{a_g} + f_g \left(1 - \frac{a_e}{a_g}\right) \qquad \text{(a11)}$$

As is usually recommended, f_g can be correlated for both the laminar and turbulent conditions, using an Ergun-type equation [9]:

$$f_g = 0.0178 + 6.2 / Re_g \qquad \text{(a12)}$$

where the constant values depend on the particular packing type, and are evaluated from analysis of the dry pressure drop measurements. In this case, we have assumed for the same values for MellapakPlus as those suggested by Brunazzi and Paglianti [9] for the Mellapak packing in metal since the surface texture is identical for both packings.

According to [9], the interfacial friction factor is evaluated by:

$$f_i = f_g\left[1 + 0.348 \cdot Bo^{0.3} + 700 \cdot \left(\frac{\delta - \delta_0}{d_e}\right)\left(\frac{\mu_l}{\mu_{l,0}}\right)^{0.15} \cdot We_l^{0.6}\right] \qquad (a13)$$

where Bo and We are the Bond and Weber numbers of the liquid phase respectively. The only difference in the expression to the relation suggested by Brunazzi and Paglianti [9] is the exponent 0.15 in the viscosity term. This correction was necessary because the original relation was developed for systems with viscosity up to 7 cP and not tested with systems of higher viscosity.

Dimensionless numbers

$$Re_g = \frac{\rho_g U_{sg} d_e}{\mu_g e \sin\vartheta} \qquad (a14)$$

$$Bo = \frac{(4\delta)^2 g\left(\rho_l - \rho_g\right)}{\sigma_l} \qquad (a15)$$

$$We_l = \frac{\rho_l V_l (4\delta)^2}{\sigma_l} \qquad (a16)$$

NOMENCLATURE

a_e	packing wetted area, m^2/m^3
a_g	packign specific area, m^2/m^3
C_G	gas capacity factor, m/s
C_L	liquid capacity factor, m/s
d_e	equivalent diameter, m
e	packing void fraction
f_i	interfacial friction factor
f_g	friction factor at channel wall
f_m	mean friction factor
F	gas load F-factor, $m/s(kg/m^3)^{0.5}$
g	gravitational constant, m/s^2
h_l	liquid hold-up
H	height of a packing element, m
L_{eq}	equivalent length of channel, m
N_c	number of flow direction changes per unit height of packing
P	pressure, N/m^2
s_g	channel perimeter dry, m
s_i	interfacial shord, m
U_{sg}	superficial velocity of gas phase, m/s
U_{sl}	superficial velocity of liquid phase, m/s
V_g	effective gas velocity, m/s
V_l	effective liquid velocity, m/s

Greek letters

δ liquid film thickness, m
δ_0 liquid film thickness measured in the absence of gas flow, m
μ_g viscosity of gas, N m
μ_l viscosity of liquid, N m
$\mu_{l,0}$ viscosity of water at 20°C, N m
ϑ packing corrugation angle, deg
π 3.14159….
ρ_g gas density, kg/m^3
ρ_l liquid density, kg/m^3
σ_l liquid surface tension, N/m
τ_{wg} shear stress at the channel wall, N/m^2
τ_i shear stress at the gas-liquid interface, N/m^2
τ_{zy} shear stress in the liquid film, N/m^2
x axial coordinate, m
y coordinate in a plane normal to z and oriented as liquid flow, m
z coordinate normal to channel wall, m

Subscripts

chan channel
d distributed
c concentrated
F frictional
G gravitational
l liquid phase
T overall

REFERENCES

1. J. G. Stichlmair and J. R. Fair (1998), Distillation. Design and Practice, Wiley VCH, New York.

2. E. Brunazzi, G. Nardini and A. Paglianti (1995), Chem. Eng. Technol., 18, 248-255.

3. G. Parkison and G. Ondrey (1999), Chem. Eng., 39-43.

4. L. Spiegel and W. Meier (1994), AIChE Spring National Meeting, paper 91C.

5. Z. Olujic, H. Jansen, B. Kaibel, T. Rietfort, E. Zich (2001), Ind. Eng. Chem. Res., 40, 6172-6180.

6. P. Suess and L. Spiegel (1992), Chem. Eng. Processing, 31, 119-124.

7. P. Marchot, D. Toye, A-M. Pelsser, M. Crine, G. L'Homme and Z. Olujic (2001), AIChE J., 47, 1471-1476.

8. E. Brunazzi, A. Paglianti and S. Pintus (2001), Ind. Eng. Chem. Res., 40, 1205-1212.

9. E. Brunazzi and A. Paglianti (1997), AIChE J., 43, 317-327.

10. J. F. Billingham and M. J. Lockett (1999), Trans. Inst. Chem. Eng., 77 (Part A), 583-587.

11. F. Moser and A. Kessler (1999), Increased capacity thanks to improved geometry, Sulzer tech. Rev. 3, 24.

12. Sulzer, MellapakPlus. A new generation of structured packings, Pubbl. No. 22.09.06.40; Sulzer, Winterthur.

13. V. Engel, J. Stichlmair and W. Geipel (1997), Inst. Chem. Eng. Symp. Ser., 142, 939-947.

14. F. Tolaini (2001), Experimental Analysis and Fluid-dynamic Modelling of MellapakPlus Packing (in italian), M.Sc. Thesis, University of Pisa, Italy.

15. W. Meier, R. Hunkeler and W. D. Stöcker (1979), Chem. Ing. Tech., 51, 119-122.

16. H. K. Kister (1992), Distillation Design, McGraw Hill.

17. Sulpak, Sulzer's column design tool, at http://www.sulzerchemtech.com

18. J.A. Rocha, J. L. Bravo and J. R. Fair (1993), Ind. Eng. Chem. Res., 32, 641-651.

19. M. G. Shi and A. Mersmann (1985), Ger. Chem. Eng., 8, 87-96.